Review Article

A review of stress concentration factors in tubular and non-tubular joints for design of offshore installations

Dikshant Singh Saini, Debasis Karmakar, Samit Ray-Chaudhuri*

Department of Civil Engineering, Indian Institute of Technology Kanpur, Kanpur, UP 208016, India

Abstract

Tubular structures are widely used in offshore installations, trusses, high rise buildings, towers for wind turbines, ski-lift installations, lightning, road pole signals etc., owing to their excellent structural performance and attractive appearance. Stress concentration, especially in the welded joints of these structures, is an important design consideration particularly for fatigue design. In the context of tubular and non-tubular joints, this paper provides a review of the experimental and numerical studies that have been carried out so far to determine the stress concentration factor (SCF). Emphasis is also placed on the complexity of capturing different types of stresses in tubular/non-tubular joints for estimation of SCF. Present code provisions for evaluation of SCF are also discussed. Further, a few issues, which require significant research effort to advance our understanding and to improve the current design guidelines, have been identified.
© 2016 Shanghai Jiaotong University. Published by Elsevier B.V.
This is an open access article under the CC BY-NC-ND license (http://creativecommons.org/licenses/by-nc-nd/4.0/).

Keywords: Hot-spot stress; Stress concentration factor (SCF); Fatigue; Tubular joints; Non-tubular joints.

1. Introduction

Three dimensional structures fabricated from steel tubular sections are widely used these days in various structures such as trusses, high rise buildings, towers for offshore wind turbines, and offshore installations. This is because the tubular sections have inherent properties of minimizing the hydrodynamic forces, and possess high torsional rigidity as well as higher strength to weight ratio compared to the conventional steel sections. Hence, from construction cost as well as strength point of view, it is advantageous to use the tubular hollow sections for various applications, especially for offshore structures.

Typically used tubular sections in offshore platforms are circular hollow sections (CHS). However, in case of truss structures, bridges and high rise buildings, rectangular hollow sections (RHS) or square hollow sections (SHS) are commonly used. A connection between two or more tubular sections is refereed as tubular joint. For a tubular joint consisting of two pipes of different diameters, the larger diameter pipe is called the chord and the smaller one is known as the brace. Figs. 1 and 2, respectively show a few uni-planar and multi-planar tubular joints that are being used in offshore structures. Non-tubular joints are those where tubular member are connected to a non-tubular section such as tubular to a girder flange, girder flange connection to a vertical tubular leg member at ring stiffener plate and girder flange to a girder flange or flange plate. Schematic diagram showing these joints are provided in Fig. 3.

Many of these structures undergo several types of cyclic environmental/operational loading e.g., wind, wave, ice and traffic loads during their service lives. As a result, fatigue damage occurs in critical joints of these structures. Stacey and Sharp [1], Chang and Dover [2] verified the data provided by U.K.'s Health and Safety Executive and identified that the fatigue was the major cause of repair to steel offshore platforms in the North Sea. The most sensitive fatigue areas in offshore platforms are the welds in tubular joints.

* Corresponding author. Fax: +915122597395.
  E-mail addresses: dikshant@iitk.ac.in (D.S. Saini),
dkarmakar@gmail.com (D. Karmakar), samitrc@iitk.ac.in
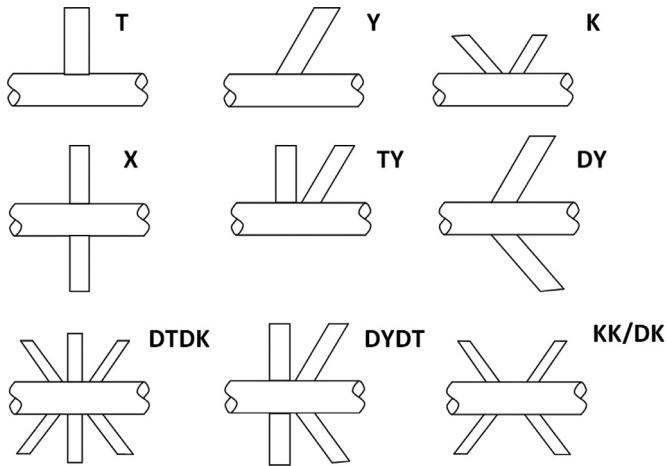 (S. Ray-Chaudhuri).

Fig. 1. Types of tubular joints along with their nomenclature.

1.1. Stress distribution in tubular and non-tubular joints

The total stress at a joint can be defined as the resultant of different stresses in the tubular/non-tubular joints as shown in Fig. 5. These are mainly due to the structural action (Nominal stress), stress arisen to maintain compatibility between different members (Geometric stress) and due to discontinuity at the joint (Local stress). A brief description of these stresses are provided as follows:

Nominal Stress: Nominal stress (σ_{nom}) can be calculated using the simple beam theory and the superposition principle without consideration of the localized weld effect and geometric discontinuity. The nominal stress can be determined as follows:

$$\sigma_{nom} = \frac{P}{A} \pm \frac{M}{I}y \qquad (1)$$

where P is the applied axial compressive load, A is the cross-sectional area, M is the applied bending moment; and y is the position of the extreme fiber.

Geometric Stress: Geometric stress (σ_G) also known as the hot-spot stress/structural stress, is used to calculate the fatigue

life of a tubular/non-tubular joints. Due to the difference in deformations between the brace and chord member of a joint, the tube wall tries to bend to maintain the compatibility and therefore, giving rise to geometric stress. This also results in the distribution of the membrane stress.

Local Stress: Local stress is caused mainly due to the local notch of the weld toe. It is a function of weld geometry and size. Thus, local stress is mainly dependent on the quality of welding and workmanship and it is quite difficult to incorporate such effects into formulation of stress concentration.

1.2. Stress concentration factor (SCF)

Fig. 4 illustrates the stress concentration phenomenon due to in-plane axial load. This figure clearly shows that local stress at the welded joint is several times higher than the nominal stress due to stress concentration. It may be noted that the local peak stresses are highly influenced by the weld profile.

There are different approaches for fatigue life analysis of a welded joint. These methods are distinguished mainly by the parameters used for the description of fatigue life 'N' or fatigue strength. These approaches include nominal stress approach, structural or hot-spot stress approach, notch stress or notch intensity approach, notch strain approach, crack propagation approach, etc. Among these, hot-spot stress is the most widely used and recommended by various fatigue design guidelines (e.g., American Petroleum Institute (API) [3], CIDECT Design Guide No. 8 [4]).

The hot-spot stress method, also known as geometric stress method, considers the stress raising effect due to structural discontinuity except the stress concentration due to weld toe, i.e., without considering the localized weld notch stress. Hot-spot stress is the surface value of structural stress at hot-spots. The hot-spots are the locations at a welded joint where the initiation of cracks is possible under cyclic loading due to increased stress value. This method was developed in 1970s by the offshore platform operators with the help of research institutes. The main aim was the fatigue strength assessment
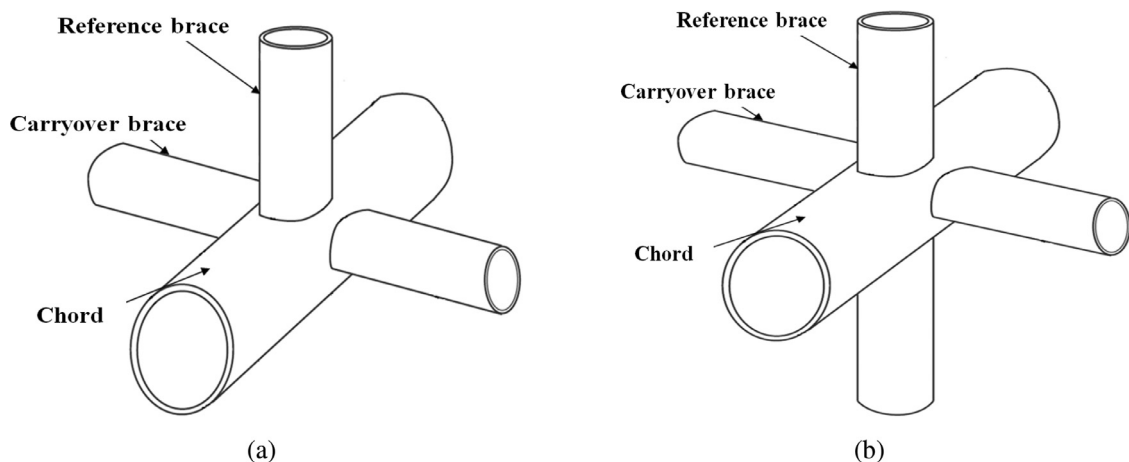

Fig. 2. Example of multi-planar joints (CIDECT Design Guide No. 8 [4]): (a) multi-planar XT joint and (b) multi-planar XX joint.
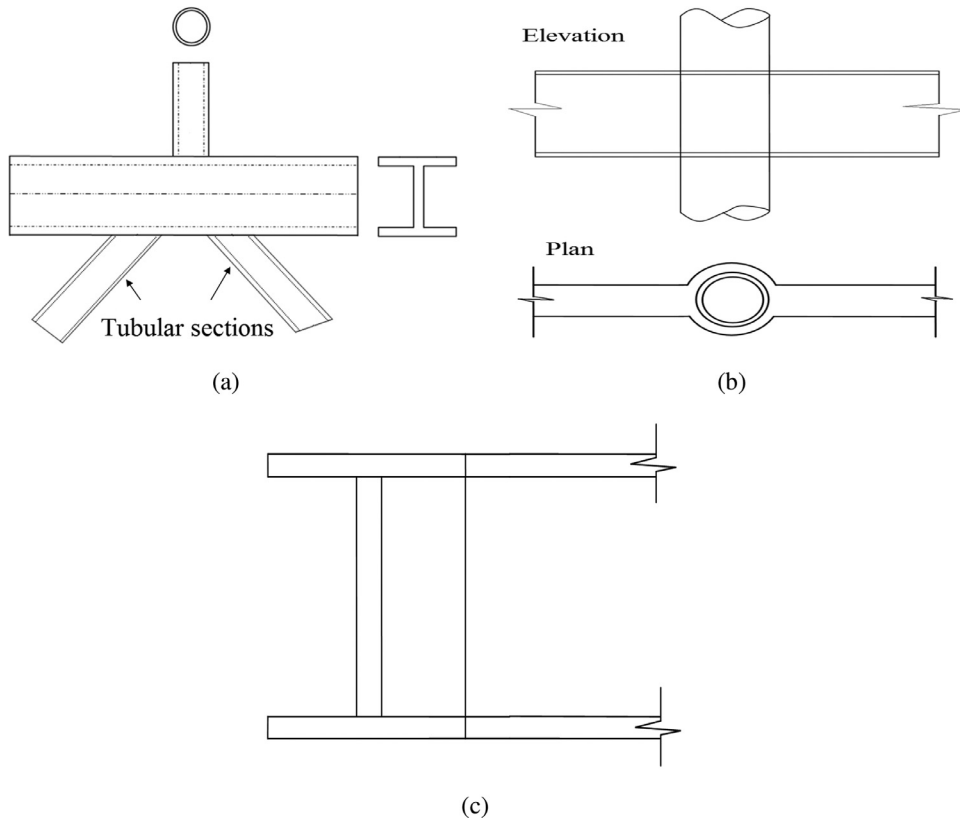
Fig. 3. Non-tubular joints: (a) Tubular to a girder (I-section) connection, (b) Unstiffened I-section to CHS connection, and (c) Girder flange to girder flange connection.
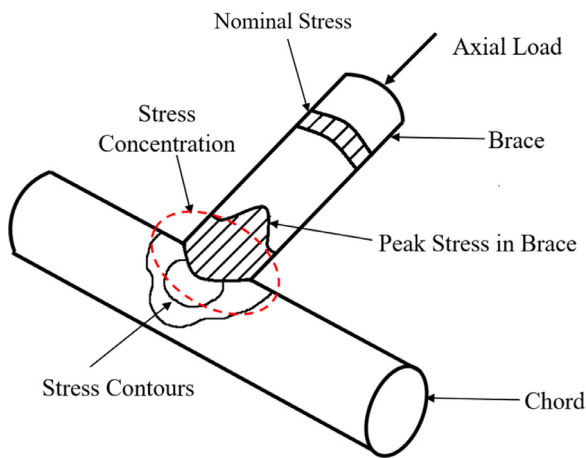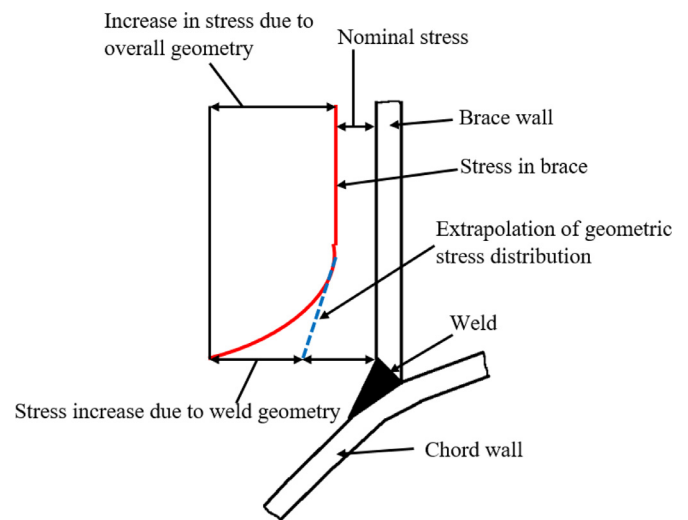

Fig. 4. Stress concentration in tubular T joint.

Fig. 5. Stress distribution in tubular/non-tubular joints.

of the tubular joints. Radaj [5] demonstrated, particularly for plate and shell structures, that the hot-spot stress corresponds to sum of the membrane and bending stress at the weld toe. These stresses can be determined either by surface extrapolation or inner liberalization of the stress. Fig. 7 provides stress distribution through the thickness of the weld plate and its components. Three components of notch stress can be distinguished from the non-linear stress distribution as shown in this figure. These are (i) membrane stress (σ_{mem}), (ii) shell bending stress (σ_{ben}), and (iii) non-linear stress part (σ_{nlp}).

The membrane stress is constant and bending stress varies linearly throughout the thickness. The remaining part is the non-linear stress part. Hence, in hot-spot stress method, the latter part (non-linear part, σ_{nlp}) is excluded from the structural stress. This is because, the exact and detailed weld profile cannot be certainly known during the design phase.

In hot-spot stress method, the fatigue life is directly related to hot-spot stress instead of the nominal stress. Fatigue life of
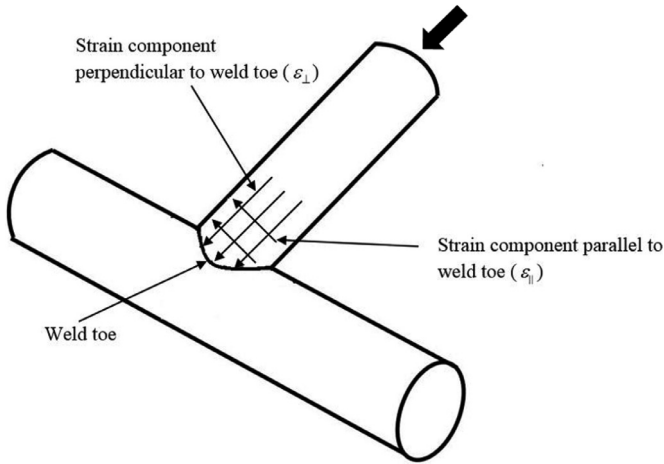
Fig. 6. Parallel and perpendicular strain components to weld toe.

tubular/non-tubular joints is usually defined using $S_{r_{hs}} - N_f$ curves. An $S_{r_{hs}} - N_f$ curve shows the relation between hot-spot stress range and the number of cycles to failure. This method gives an advantage over the other methods as a reduced number of $S_{r_{hs}} - N_f$ curves are needed to evaluate the fatigue life of welded details by the stress concentration factors. The fatigue life performance of tubular/non-tubular joints is also dependent on thickness of the structural members. The fatigue life of tubular/non-tubular joints gets reduced as the thickness of the structural member increases. This effect, also known as thickness effect, is accounted in the $S_{r_{hs}} - N_f$ curves by multiplying the stress range with a thickness correction factor. Significant research has been done to incorporate the thickness effect. These corrections are included in many guidelines including American Petroleum Institute (API) [3], CIDECT Design Guide No. 8 [4] and IIW (Hobbacher [6]).

In hot-spot stress approach, the ratio of the hot-spot stress (σ_{hss}) and the nominal stress (σ_n) in an attached brace/chord is defined as the stress concentration factor (SCF) and is expressed as follows:

$$SCF = \sigma_{hss}/\sigma_n \tag{2}$$

Generally, one member (brace/chord) is loaded at a time while evaluating SCF. If chord or other members are also loaded along with the brace member in a joint, additional hot-spot stresses are generated. For simultaneous loading in chord and brace members, a more general definition of SCF is adopted. In such cases, hot-spot stress (HSS') is the function

of all nominal stresses in all the brace/chord members as given here:

$$HSS' = \sum_k (SCF)_k \Delta\sigma_{nom}^k \tag{3}$$

where $(SCF)_k$ implies the component of stress concentration factor for nominal stress $\Delta\sigma_{nom}^k$ due to loading type (k).

In case of experimental evaluation, SCFs are actually calculated on the basis of corresponding strain components. This is because the hot-spot strain can be directly measured with the help of strain gauges. In earlier studies, SCFs have been determined by using both principal stress and the stress perpendicular to the weld toe. Wingerde et al. [7] favored the stress perpendicular to the weld toe rather than the principal stress for calculating SCFs. This is because (a) the difference between the stress perpendicular to weld toe and the principal stress is small near the weld toe, (b) the strains perpendicular to weld toe can be measured easily by simple strain gauge as compared to strain rosettes to measure the principal strains, and (c) the direction of the principal stress will be different for different load cases. Two strain components are required for calculating the SCF. These are: (i) the hot-spot strain component parallel to weld toe $\xi_\parallel$ and (ii) the hot-spot strain component perpendicular to the weld toe $\xi_\perp$ (see Fig. 6). The relationship between SCF and strain concentration factor (SNCF) can be expressed as:

$$SCF = \frac{1 + \nu\frac{\xi_\parallel}{\xi_\perp}}{1 - \nu^2} SNCF \tag{4}$$

where SNCF is defined as

$$SNCF = \xi_\parallel/\xi_n \tag{5}$$

In Eqs. (4) and (5), ξ_n and ν are the nominal strain and Poisson's ratio, respectively. The ratio of SCF to SNCF is known as the S/N ratio. Thus, the location of hot-spots has to be well defined for evaluating the SCFs of a joint.

1.3. Mesh insensitive structural stress method

In order to estimate more reliable design lives of tubular and non-tubular joints, a more consistent procedure to estimate SCF is needed. Dong [8] utilized the definition of structural stress given by Radaj [5] and developed a robust structural stress method insensitive to mesh size. This method provides more reliable hot-spot stress estimation and information

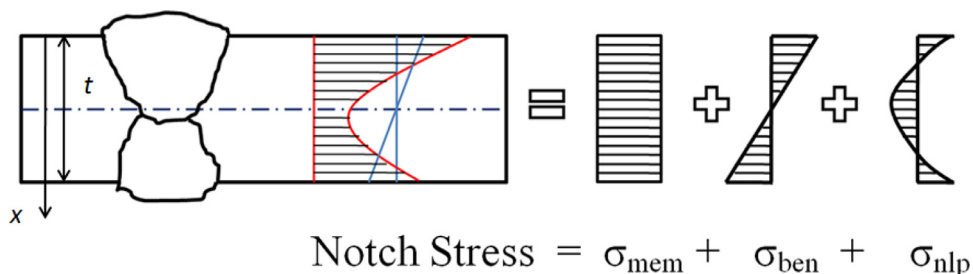$$\text{Notch Stress} = \sigma_{mem} + \sigma_{ben} + \sigma_{nlp}$$

Fig. 7. Stress distribution through the thickness of the weld plate and its components.

needed for fatigue life estimation using fracture mechanics. A master *S-N* curve is established for a wide variety of joints including typical tubular joints. In this method, the structural stress is calculated using the nodal (internal) forces from the finite element solution. The structural stress is calculated as the sum of membrane stress and bending stress (same as defined by Radaj [5]). The expression for these stresses are provided as follows:

$$\sigma_{mem} = \frac{1}{t} \int_{x=0}^{x=t} \sigma(x) dx \qquad (6)$$

$$\sigma_{ben} = \frac{6}{t^2} \int_{x=0}^{x=t} (\sigma(x) - \sigma_{mem})\left(\frac{t}{2} - x\right) dx \qquad (7)$$

$$\sigma_{nlp} = \sigma(x) - \sigma_{mem} - \left(1 - \frac{2x}{t}\right)\sigma_{ben} \qquad (8)$$

where *x* and *t* are shown in Fig. 7. Dong and Hong [9] presented applications of structural stress procedure for evaluating SCF of tubular joints such as CHS T, double T, YT joints with overlap and K joints with various internal stiffening configurations. The SCF evaluated using structural stress method showed no noticeable variability for the tubular joints investigated. The structural stress method was found to be far more effective than conventional hot-spot stress method in collapsing down the *S-N* curve data onto a narrow band. Liu et al. [10] demonstrated the use of structural stress method, and calculated the structural stress for the fatigue life of a tubular T joint. The basic difference between the HSS method and mesh insensitive structural stress method is that the HSS method fails to consider the stress distribution in the wall thickness direction. Another advantage of this method is that the degree of bending (DoB) (which is required for fracture mechanics calculations) is directly available.

1.4. Extrapolation methods

Since hot-spot stress method does not account for stress raising effect due to welding and local conditions of the weld toe, the hot-spot stress cannot be determined directly by putting the strain gauge near the weld toe. Rather, a fictitious value of hot-spot stress is used based on extrapolation points, which are at certain distance away from the weld toe (as shown in Fig. 8). These extrapolation procedures are defined in prevalent design guidelines such as CIDECT Design Guide No. 8 [4] and IIW [11]. These guidelines are based on the geometric strains outside the chord and brace intersections. The location from which the strains are extrapolated depends on the dimensions of the joint and the boundaries for the extrapolated region.

Department of Energy [12] defined the maximum extent of local notch stress region as $0.2(rt)^{1/2}$ (for $t \geq 4$ mm) based on the bending stresses in the tubes, where *r* and *t* are the brace outer radius and thickness, respectively. American Welding Society (AWS) [13] and American Petroleum Institute (API) [14] recommended a region within 6 mm to $0.1\sqrt{rt}$ from
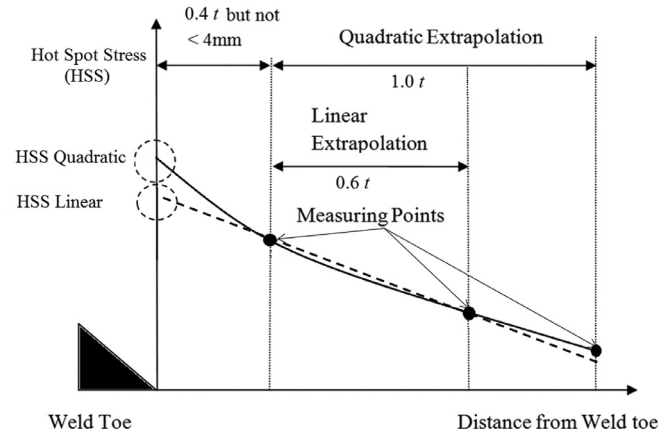

Fig. 8. Methods of extrapolation to the weld toe (CIDECT Design Guide No. 8 [4]).

Table 1
Extrapolation methods recommended by CIDECT Design Guide No. 8 [4] and IIW [11].

Distances from weld toe	CHS chord member		CHS brace member
	Crown	Saddle	Crown and Saddle
$L_{r, min}$	$0.4T$		$0.4t$
$L_{r, max}$	$0.4\sqrt[4]{rtRT}$	$0.09R$	$0.65\sqrt{rt}$
	RHS chord member		RHS brace member
	Crown	Saddle	Crown and Saddle
$L_{r, min}$	$0.4T$		$0.4t$
$L_{r, max}$	$L_{r,min} + T$		$L_{r,min} + t$

Minimum value of $L_{r, min}$ is 4 mm
Minimum value of $L_{r, max}$ is $L_{r,min} + 0.6t$

the weld toe for the strain measurement. Based on the finite element analysis of fillet welded joints in plates, Gurney [15] proposed an alternative approach and recommended a minimum gauge distance of $0.4t$ from the weld toe. Wardenier [16] commented that Gurney's recommendations are better in defining the notch for joints with pronounced three dimensional effect. Furthermore, ECSC [17] adopted the recommendations given by Gurney [15] in their guidelines. Later on, the aforementioned extrapolation procedures were also included in the design guidelines [3,4,11].

The extrapolation boundaries as given in the present CIDECT Design Guide No. 8 [4] for the circular hollow section (CHS) and rectangular hollow section (RHS) are defined in Table 1 and Fig. 9, where *R* and *T* are the outer radius and thickness of the chord, respectively. Two extrapolation methods are defined for determination of HSS. These are: (i) linear and (ii) quadratic (see Fig. 8). CIDECT Design Guide No. 8 [4] have proposed that the quadratic extrapolation procedure is required for square and rectangular hollow sections, whereas the linear extrapolation method is required for circular hollow sections. This is because of high non-linear strain distribution in SHS/RHS joints as compared to CHS joints. Both extrapolations can be done by fitting the curve manually or numerically. For linear extrapolation, at least two points are
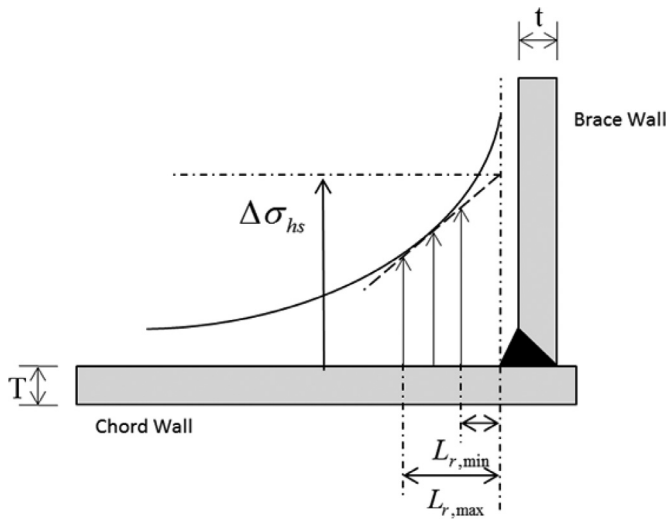
Fig. 9. Definition for extrapolation region (CIDECT Design Guide No. 8 [4]).

required on the curve. The first point of extrapolation is $0.4t$ from the weld toe but not less than 4 mm, where t is the thickness of tubular members. The second point is $0.6t$ away from the first point. For the quadratic extrapolation, a minimum of three points are required. The first point of extrapolation is $0.4t$ from the weld toe but not less than 4 mm. The second and third points are respectively, $0.6t$ and $1.0t$ away from the first point.

For the non-tubular or plated structures, many fatigue guidelines have provided different methods for the determination of hot-spot stress using finite element methods. A brief description of these methods or guidelines is provided here. Det Norske Veritas (DNV) [18] recommended linear extrapolation where the principal stress is to be calculated at a distance of $t/2$ and $3t/2$. A mesh size of $t/2 \times t/2$ for the 20-node solid elements, and a mesh size of $t \times t$ for the 8-node shell elements have been recommended. Fricke et al. [19] recommended 20-node solid element with a mesh size equal to the thickness of the plate, where three elements of equal size are to be used in the area of high strain gradient. Quadratic extrapolation is needed to performed with the calculated stress on the upper surface from 4 integration points (i.e., edge nodes of three elements). Fricke [20] along with a special task group investigated the hot-spot stresses in structural details of floating production, storage and offloading units (FP-SOs) as well as in ships using finite element (FE) methods. Various FE models with different elements, mesh sizes, stress evaluation techniques, and using different FE programs were developed. The main objective was to identify how to predict accurately the hot-spots stresses and to correlate the stress extrapolation with the available *S-N* curves. These FE models can be broadly classified as plate/shell models and solid element models. It was recommended that plate/shell models offer simplified modeling with 8-node elements in areas of higher stress gradient. Weld geometry need not be modeled except in case of high local bending. In case of complex geometries, it was recommended to use the 20-node solid elements with weld profile. Fricke [20] also provided mesh size recommendation and stress evaluation points for the calculations of hot-spot stress. These recommendations were almost similar to as those given in Fig. 10 and Table 2. American Bureau of Shipping (ABS) [21] recommended a mesh size of $t \times t$ for both the 20-node solid and 8-node shell elements. Linear extrapolation was recommended with maximum principal stresses calculated at $t/2$ and $3t/2$. IIW (Hobbacher [6]) gave recommendations on fatigue of welded components and structures with an emphasis on hot-spot stress method. This
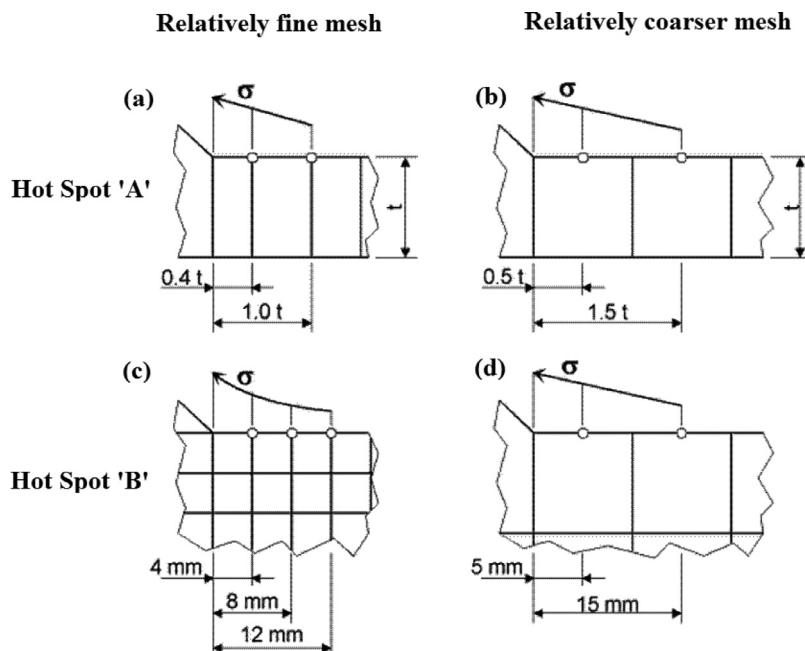

Fig. 10. Reference points for extrapolation (IIW (Hobbacher [6])).

Table 2
Mesh size recommendations IIW (Hobbacher [6]).

Element type and Mesh size		Relatively coarser mesh		Relatively finer mesh	
		Type A	Type B	Type A	Type B
Element size	Shells	$t \times t$ (max $t \times w/2^*$)	10×10 mm	$\leq 0.4t \times t$ $\leq 0.4t \times w/2$	$\leq 4 \times 4$ mm
	Solids	$t \times t$ (max $t \times w$)	10×10 mm	$\leq 0.4t \times t$ $\leq 0.4t \times w/2$	$\leq 4 \times 4$ mm

* w = longitudinal attachment thickness + 2 × weld leg lengths.

Table 3
Parametric equations for SCFs.

| Authors	Joint types	Derived from	Remarks
Kuang [23]	T/Y, K and KT	FEA	HSS only
Wordsworth and Smedley [24,25]	T/Y, K (gap and overlap), X and KT	Acylic model test	HSS only
UEG [26]	T/Y, K (gap and overlap), X and KT	FEA and Test data	HSS only
Efthymiou/Durkin [27,28]	T/Y, K and KT	FEA	HSS and Influence functions
Hellier, Connolly and Dover [29]	T/Y	FEA	HSS, DOB and Distributions
Smedley and Fisher [30] (Lloyd's Register)	T/Y, X, K and KT	Steel and acrylic model test	HSS and Influence functions
Morgan and Lee [31–33]	K and KT	FEA, Steel and acrylic model test	HSS, DoB and Distributions
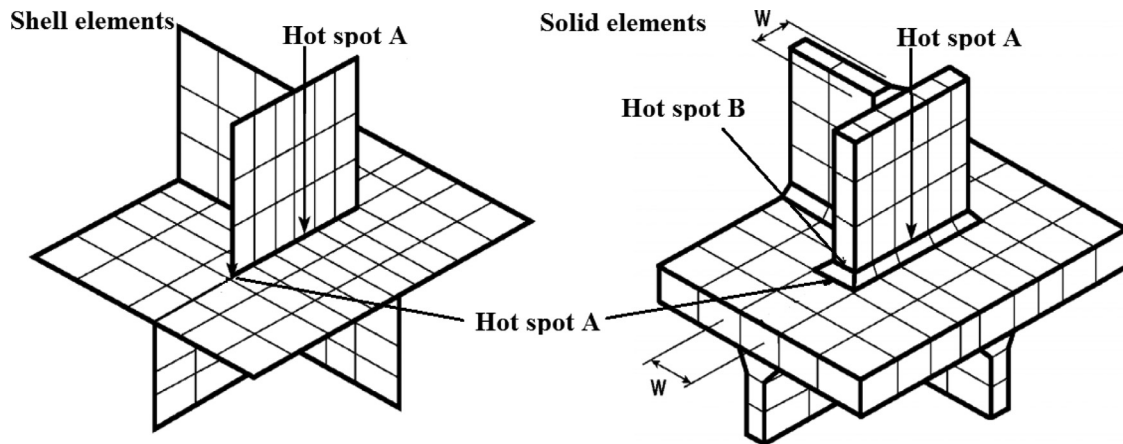
Fig. 11. Typical meshes and hot-spot locations for weld details (IIW (Hobbacher [6])).

includes guidelines for numerical analysis using finite element methods to determine and validate hot-spot stress method. IIW (Hobbacher [6]) defines two types of hot-spots (Fig. 11): (i) hot-spot A (weld toe on the plate surface), and (ii) hot-spot B (weld toe on the plate edge). Based on the type of hot-spot, different recommendations for finite element mesh size and points of extrapolation are provided in IIW (Hobbacher [6]) as shown in Fig. 10 and Table 2. A more detailed description of hot-spot stress procedure for experimental or numerical analysis can be found in the IIW (Hobbacher [6]).

1.5. Parametric equations

The hot-spot stress method requires an accurate prediction of SCFs. Toprac and Beale [22] presented the earliest set of parametric equations to determine SCF in simple tubular joints using a limited steel joint database. During the past 50 years, several parametric equations have been proposed by researchers for determining the hot-spot stress. In the next section, a brief description of the commonly used parametric equation is provided with an emphasis on how the hot-spot stress is defined and their range of applicability. In the following section, several non-dimensional geometric parameters are defined (refer to Fig. 12 for their definitions).

1.5.1. Kuang equations

Kuang et al. [23] established parametric equations to determine SCFs for T/Y, K and KT tubular joints based on thin shell finite element analysis. The joint was divided into several regions and mesh refinement was done in four layers.
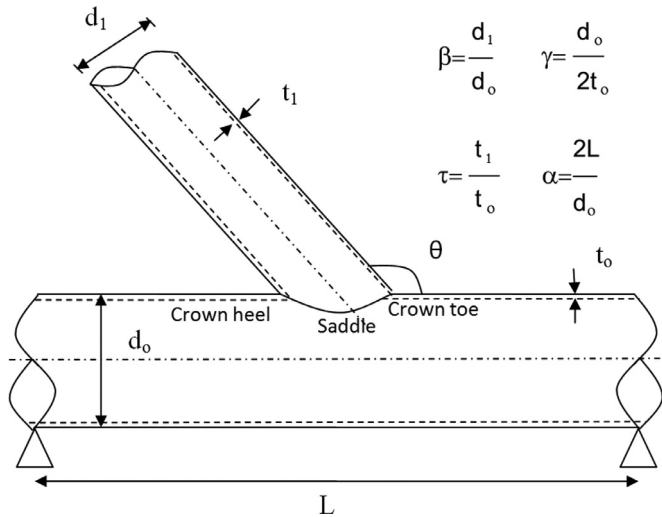
Fig. 12. A uni-planar CHS T or Y joint (CIDECT Design Guide No. 8 [4]).

The weld profile was not considered, and the stresses were measured at the mid-section of the member wall without extrapolation. This simplification led to underestimation of SCF. These equations are only expressed as chord-side and brace-side and are not indicative for a specific location. These equations are limited to fewer joints in the database. These equations do not cover joints with $\beta > 0.80$ and do not cover X joints. For K and KT joint configurations, no equations were given for unbalanced OPB loading. For T/Y joint under axial loading, these equations didn't account for the beam bending effect, which may lead to underestimations of SCF for high α values. For the T joints configuration in the range $0.5 < \beta \leq <0.8$, the performance of Kuang et al. [23] equations is generally poor. For the KT joints, the measured SCF was found to be four times larger than the measured SCF values[30].

1.5.2. Wordsworth/Smedley equations

Wordsworth and Smedley [24] and Wordsworth [25] derived equations for T/Y, X, K and KT joints using acrylic model test on tubular joints. The weld profile was excluded from the model and strains were measured using the strain gauges at different locations. Wordsworth and Smedley [24] gave SCFs for simple T/Y and X joints under axial, IPB and OPB loading. These equations covered only the saddle and crown locations of the welds and no information was provided for the interim positions. Wordsworth [25] presented parametric equations to calculate SCFs for K and KT joint under axial, IPB and OPB loading. These equations were again based on acrylic model tests. Wordsworth [25] considered a K or KT joint as a combination of T or Y joint on which additional braces were added. Aforementioned parametric equations were restricted to planar tubular joint configurations and specific types of planar tubular joints i.e., T/Y, X, K and KT joints. Furthermore, they were restricted to specific combinations of brace loading in case of K, KT, and X joints. For joint configurations with equal chord and brace diameters ($\beta = 1.0$), a value of $\beta = 0.98$ was proposed to

approximate the weld cut back at the saddle location. It is almost impossible to match brace and chord surface tangentially i.e., there is some degree of cut back. As a result of this cut back, the load transfer between brace and chord is less efficient, and the HSS increases. Under axial loading and OPB at the saddle location, these equations tend to underestimate the SCFs on joints with $\beta = 1.0$ and high γ.

1.5.3. UEG equations

UEG [26] proposed parametric equations based on Wordsworth and Smedley [24], Wordsworth [25] using minor modification factor. This modification factor was introduced to accurately predict the SCF with joint configurations ($\beta > 0.6$, $\gamma > 20$) as shown in Fig. 12. The modification factor was derived by comparing the predicted and measured results for static as well as fatigue tests. The two factors $\sqrt{Q'_\beta}$ and $\sqrt{Q'_\gamma}$ are applied under axial load and OPB. For IPB, the factor $\sqrt{Q'_\gamma}$ is applied. The expressions for Q'_β and Q'_γ are as follows:

$$Q'_\beta = 1.0 \quad \text{for } \beta \leq 0.6 \tag{9}$$

$$Q'_\beta = 0.3/\beta(1-0.833\beta) \quad \text{for } \beta > 0.6 \tag{10}$$

$$Q'_\beta = 1.0 \quad \text{for } \beta < 20 \tag{11}$$

$$Q'_\beta = 480/\gamma(40-0.833\gamma) \quad \text{for } \beta \leq 20 \tag{12}$$

1.5.4. Efthymiou/Durkin equations

Efthymiou and Durkin [27] derived SCF equations for T/Y and K joints using PMB SHELL finite element program. The weld profile around the brace chord intersection was considered. Although hot-spot stress method was used for the evaluation of SCFs, the results were observed to be affected by the contribution of fillet weld in the joint stiffness. Efthymiou [28] published a set of parametric equations for prediction of SCFs of T/Y, X, K and KT joints based on the maximum principal stress rather than the stress perpendicular to the weld toe. These equations were developed using the influence functions to predict the SCF of K, KT, and multi-planar joints in terms of simple T joint with carry-over effect from additional braces. Equations proposed by Efthymiou [28] predicted maximum SCFs at the weld toe of the chord and the brace, and were independent of the chord end boundary conditions. It was also shown by Efthymiou [28] that the saddle SCF is reduced in joints with short chord lengths. This is due to the fact either the presence of chord end diaphragms or the rigidity of the chord end fixing onto the test rig restricts the chord ovalisation. Efthymiou equations underpredict the SCF on the vertical brace under OPB loading for K joints with one vertical brace and one inclined brace. The K joint equations were developed with more emphasis on the overlapped K joint as compared with gap K joint. Therefore, the equations for gap K joints may not give reliable estimates. Although these equations were derived based on mean fit to a database of finite

element tubular joints examined, under-prediction of SCF using these equations was reported in later studies. It may however be noted that these equations are widely accepted and used in offshore industries. In fact, SCF equations proposed by Efthymiou [28] are included in American Petroleum Institute (API) [3]. The main limitation of this work is that the SCF equations were given only for few locations around the intersection.

1.5.5. Hellier, Connolly and Dover equations

Hellier et al. [29] proposed SCF equation for T/Y joint with an objective of improvement in the prediction of fatigue life of tubular joints based on fracture mechanics. An extensive finite element analysis of tubular joints was carried out using thin-shell elements subjected to axial load, in-plane and out-of-plane bending. The proposed equations for estimating SCF were found to be applicable for joints with $\beta < 0.8$. A thin-shell finite element program was used to determine SCF using the PAFEC package. Similar to Kuang et al. [23], the filled weld was not modeled in the joint models and hence, the stresses were calculated at the node without any extrapolation. The equations were derived from the thin shell FE results database at various locations, which relates the SCF to the geometric ratios of the tubular joints. The SCF estimated from proposed equations were compared with experimental results from steel models and also with three other sets of existing parametric equations. The equations were found to overestimate the SCF as compared with the experimental results while providing the most conservative SCF estimates, when compared with the other parametric equations. In addition to SCF equations, equations for DoB (ratio of bending stress to the total stress) were also developed. The DoB equations were found to be in good agreement with the acrylic model test results. The proposed SCF equations did not cover joints with $\beta > 0.8$, which limits their applications in offshore industries. However, these SCF equations can be used to obtain a useful approximation of the stress distribution around the intersection. The proposed DoB equations also provided good estimate of through thickness stress distribution, which can be used to predict the fatigue life of a tubular joint.

1.5.6. Lloyd's register equations

Lloyd's Register (www.lr.org) derived parametric equations based on tests performed on 69 acrylic and steel joints [30]. These equations only cover SCF at crown and saddle points, and do not account for maximum SCF at the joint intersection. In addition, these equations consider the short chord effects proposed by Efthymiou [28], which were not independently verified. UK Health and Safety Executive [34] report prepared by Lloyd's Register provided a comprehensive assessment of existing parametric equations for simple tubular joints. It also covered the new set of parametric equations developed by Lloyd's Register. These new equations were based on experimental investigation on steel and acrylic tubular joint specimens. A review on experimental and numerical modeling techniques to determine SCF in simple tubular joints were

also provided in this report. The joints with geometric parameters having applications in offshore platforms were included in the database i.e., $\tau \leq 1.05$, γ, ≤ 40, SCFs ≥ 1.5, $\beta \leq 1.0$. Further, Lloyd's Register prepared a report UK Health and Safety Executive [35], which covers the experimental database of SCF in multi-planar K and KK/DK joints. These equations have a limited scope and the SCF values are given only at crown and saddle points. These equations are based on 69 acrylic and steel joint specimen only, and as a result, the SCF values may not be reliable in many cases. However, these equations are well suited to estimate the fatigue life using *S-N* approach.

1.5.7. Morgan and Lee equations

Morgan and Lee [31–33] proposed a set of SCF equations for wide range of K joint configuration under axial, in-plane and out-of-plane loading. A finite element analysis using thin-shell elements was performed to calculate the stress at the mid-wall thickness of the members. On comparing the SCF measured from steel and acrylic tubular joints specimens, it was found that the Morgan and Lee equations [31–33] perform better than Efthymiou [28] and Lloyd's Register equations [30]. The parametric equations were derived for SCFs and DoBs at various locations around the weld on the chord and brace side (0°, 45°, 90°, 135° and 180°). These equations cover the full range of geometric parameters that are possible in practice.

2. SCFs at typical tubular/non-tubular joints

In this section, experimental and numerical investigations on typical tubular and non-tubular joints to evaluate SCFs are discussed in detail.

2.1. SCFs at welded T joints in circular hollow sections (CHS)

Fig. 12 shows the geometric parameters and the critical locations for stress concentrations for CHS T/Y joints (CIDECT Design Guide No. 8 [4]). Buitrago et al. [36] developed parametric equations for Y and gapped K joint using the program of Kuang et al. [23] for finite element analysis. However, the influence factors were given as a function of joint geometry and load case at hot-spot locations. Dijkstra et al. [37] determined the SCFs in a tubular T joint using finite element method (FEM) under the basic loads such as axial load or bending moment in one of the braces of the tubular T joint. The finite element analysis was carried out using a FEM program DIANA [38]. Quadratic, super-parametric and doubly curved thick shell elements were used for modeling. The results for in-plane bending and axial load on the brace of T joint were found to be comparable with the results obtained from parametric formulae proposed by Kuang et al. [23], Wordsworth and Smedley [24] and Efthymiou [28]. Based on this study, Dijkstra et al. [37] concluded that thick shell elements in the finite element analysis give good results although real weld profile should be considered along the axis.

Mashiri et al. [39] studied the fatigue behavior of thin-walled T joints consisting of both CHS braces and chords under cyclic in-plane bending. Thicknesses of brace and chord sections were less than 4 mm. Under in-plane bending, the chord and brace crown positions were found to be the hot-spot locations in CHS-CHS T joint where the measurements were taken. Strip strain gauges consisting of five strain-sensitive grids were used to study the nature of stress gradient close to the weld toes. Six different joints were tested and the stress perpendicular to the weld toe was computed at the hot-spot locations. Further, experimentally found SCFs were compared with the SCFs obtained using the parametric equations for CHS-CHS T joint from IIW [11]. It can be noted from the comparative study that the experimentally obtained SCF values were much lower than the SCFs derived from the parametric equation (IIW [11]). For example, from experiments the SCF at the chord crown position for one specimen was found to be 1.68, which is much lower than 4.48 as derived from IIW [11] equations. The ratio of experimental SCFs to the SCFs derived from the parametric equations (IIW [11]) for chord crown positions had a mean value of 0.42. Whereas, in case of brace crown positions, this value was equal 0.33. The possible reasons for obtaining such low SCF values from experiments were identified as (i) the oversized weld leg length leading to lower stress region around the weld toe and (ii) overestimation of the distance of extrapolation resulting in low stress gradient.

N' Diaye et al. [40] studied the stress concentration in welded and notched tubular T joint under axial, bending and dynamic loading. The SCFs were found to be higher under dynamic loading than static loading. Hence, they concluded that the increase of SCF under dynamic loading will further trigger the fatigue damage in the joint. They also studied the effect of notched fillet weld on the SCF. It was concluded from their investigation that notched fillet weld slightly reduces SCF on the brace member but a significant reduction was found on the chord member.

Yong-Bo [41] studied the effect of geometric parameters on the stress distribution for tubular T and K joint under brace axial loads. It was found from their study that chord thickness is an important factor, which dominates the stress distribution in both T and K joint. The brace thickness was found to have negligible effect. The parameter β was found to have different effects on the stress distribution for tubular T and K joint.

Chen et al. [42] investigated the stress concentration phenomena in concrete filled tubular T joints subjected to axial loads and in-plane bending. Five concrete filled tubular T joint along with three hollow tubular T joints were tested. The SCFs were found to be reduced under both axial loading and in-plane bending except the peak SCFs on brace under in-plane bending. However, the SCF variation in hollow tubular T joint and concrete filled tubular T joint was found similar.

In order to carry a larger load and to provide a longer life, the joints are usually stiffened using internal stiffeners or by externally reinforcing these with the help of plates. This approach also protects the tubular joints against punch-ing shear failure. Ramachandra Murthy et al. [43], Nwosu et al. [44] investigated the stress concentration and its distribution in internally stiffened tubular T joint. The stiffeners were found to reduce the stress concentration in joints considerably. Myers et al. [45] studied the effect of three different longitudinal stiffeners on the SCF of tubular T joint. For every stiffener, the SCF was found to decrease as compared with the unstiffened tubular joint. The constant-thickness continuous stiffener was found to perform well as compared with the dual thickness stiffener and the non-continuous stiffener. The SCF under IPB was found to be unaffected with the introduction of internal stiffeners. However, a maximum reduction of 50% and 20% was found under axial and OPB loadings, respectively. Fung et al. [46] studied the stress concentration factor in a doubler plated reinforced tubular T joint under axial tension, axial compression, and in-plane and out-of-plane bending. Doubler plates are commonly used to strengthen the tubular joints against the punching shear failure. They found that the ultimate load capacity of reinforced joint is higher than the normal joint. In addition, the SCF were found to be lesser for the reinforced joint than the simple joint. They also proposed that further studies should be done about the cracking through the weld connecting the doubler plate to the chord member. From this research, it is envisioned that SCF can be reduced in tubular/non-tubular joints without any adverse effects in the structure. Nazari et al. [47] carried out parametric study for tubular T joints reinforced with doubler plates using finite element analysis. Tubular T, Y, K, X and DT joints reinforced with and without doubler plates were studied in this study. The analysis results were found in good agreement with the existing parametric equations.

2.2. SCFs at welded thin walled SHS-SHS T joints

Joints of SHSs are more vulnerable to stress concentrations as compared to the circular hollow section joints. Mashiri et al. [48] carried out tests on welded thin-walled ($t < 4$ mm) T joints (SHS-SHS) under cyclic in-plane bending. In Fig. 13, a SHS-SHS T joint along with the hot-spot locations (considered by Mashiri et al. [48]) is shown. Different modes of failure were observed during these tests, namely (i) chord-tension-side failure, (ii) chord-and-brace-tension-side failure, (iii) brace-tension-side failure, and (iv) chord-compression-side failure. Cracks were initiated in the chord where the maximum SCF occurred. The experimentally obtained SCFs were compared with SCFs derived from the parametric equations (CIDECT Design Guide No. 8 [4] and IIW [11]) and found to be significantly lower than SCFs from parametric equations. From experiments, the critical SCF under in-plane bending was 11.94 as compared to 30.55 as derived from IIW [11]. The possible reasons for those very high SCF values were stated as (i) the oversized weld and (ii) the fixed point of extrapolation i.e., 4 mm for members having wall thickness (<10 mm).
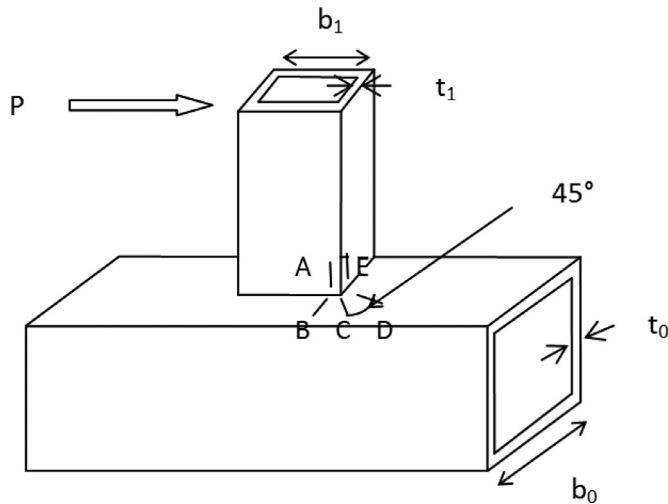
Fig. 13. Lines for strain measurement in SHS-SHS T joint (Mashiri et al. [48]).

2.3. SCFs at welded CHS-SHS/CHS-RHS T joints

T joints of welded hollow sections, e.g., CHS-SHS/CHS-RHS offer advantages in comparison to CHS-CHS, CHS-RHS and RHS-RHS. For example, CHS-SHS/CHS-RHS joints are easy and cheaper to manufacture as no profiling of the brace member is required in comparison to CHS-CHS T joints. Bian and Lim [49] conducted experimental studies on CHS-SHS/CHS-RHS joints. The static and fatigue behavior of eight CHS-RHS T joints under axial and in-plane loads were investigated by conducting experiments. The joints had a circular brace member and rectangular chord member. Based on the preliminary results, it was considered that the hot-spot locations under axial loading and in-plane loading can be considered at 45°. The measured SCF values obtained from experimental studies were found to be consistently lower than the SCF derived from the parametric equations for RHS-RHS T joint.

Mashiri et al. [50] carried out fatigue tests on tubular T joint under in-plane bending in the brace. The joints were composed of thin walled sections having circular brace member and square chord member. The SCF values for welded

CHS-SHS tubular T joint were compared with the available parametric equations (IIW [11]) as well as the experimental results for CHS-CHS and CHS-SHS T joint (Mashiri et al. [39], 48]). Fatigue cracks initiated at the weld toe of SHS chord member, which showed that the SCFs on the SHS chord were greater than the SCFs on the CHS brace member. SCFs were determined around the weld toes in the chord. As shown in Fig. 14, the lines at 0°, 45°, 60° were considered as the hot-spot locations. It was reported that the maximum SCF at the weld toes in the chord of welded thin-walled CHS-SHS T joint were 0.38 times the maximum SCF derived from the parametric equations of SHS-SHS T joint. A quadratic extrapolation was recommended by the authors for determination of hot-spot stresses at the weld toes in the chord. The authors also recommended that the lines at 0°, 30°, 45°, 60°, and 90° should be considered as the hot-spot locations near the weld toes for welded CHS-SHS T joints. This is because the hot-spot location in CHS-SHS tubular T joints depends on the β values (as defined in Fig. 14). The hot-spot location changes from 0° at low β values to 60° at relatively high β values.

Tong et al. [51] tested eight CHS-SHS T joints under axial loading and in-plane bending with unique non-dimensional parameters. The measured SCF values were found to be consistently lower than the SCF obtained by previous researchers for SHS-SHS T joint. The maximum SNCFs were found to occur at 90° in the brace and, at 0° and 90° in the chord under axial loading in the brace (Fig. 14). Further, under in-plane bending in the brace, the maximum SNCFs were found at either 0° or 60° in the brace and, either 0° or 45° in the chord (Fig. 14). The S/N ratio was found to be 1.15 and 1.2 for the brace and chord, respectively. They also carried out parametric study to establish an equation between the SNCF and geometric parameters from the verified finite element model.

2.4. SCFs at tubular X joints

Feng and Young [52] experimentally and numerically investigated the SCFs of cold formed stainless steel SHS and RHS tubular X joints. The SCFs were determined under static loading using the strip strain gauges at hot-spot locations as shown in Fig. 15. Quadratic method of extrapolation was used for the strain components parallel and perpendicular to the
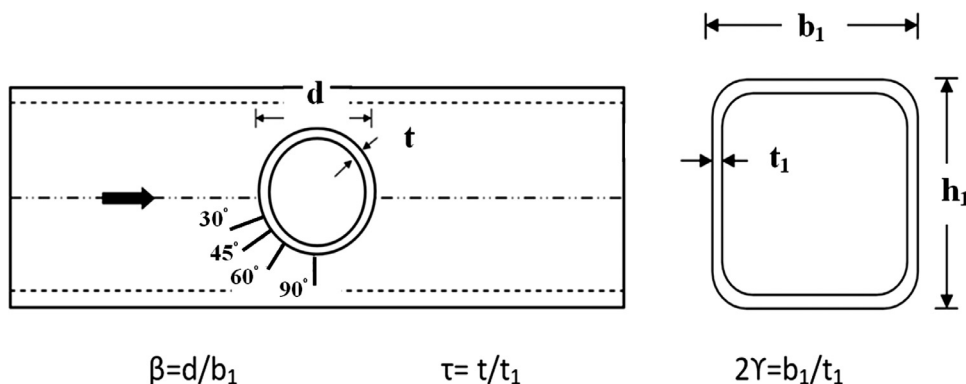

Fig. 14. Hot-spot locations in CHS-SHS tubular T joint (Mashiri et al. [50]).
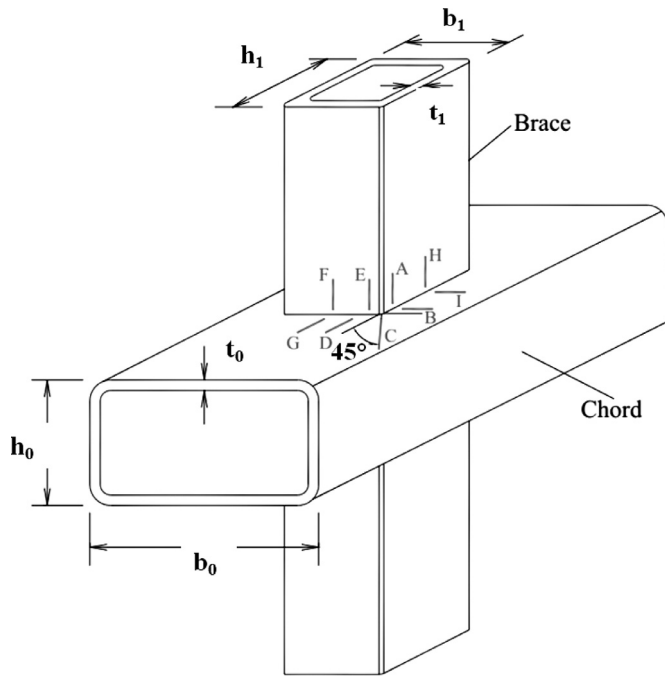
Fig. 15. Hot-spot strain measurement positions for tubular cold formed X joint (Feng and Young [52]).

Fig. 16. K(N) joint: (a) Gapped tubular K joint (Karamanos et al. [57]) and (b) Completely overlapped tubular K joint (Gho et al. [58]).

weld. It was concluded that the strain gauges can be placed as close as possible to the weld as the weld profile has little influence on the stress concentrations. Finite element analysis was performed to simulate the stress distribution along the brace and chord intersection region. Good agreement between the finite element results and the experimental results was achieved. Based on the verified finite element model, an extensive parametric study was carried out to evaluate the effects of parametric variations on the SCFs of cold formed stainless steel tubular X joints. A design equation was proposed for calculation of SCFs at typical hot-spot locations based CIDECT Design Guide No. 8 [4] and the study by Wingerde et al. [7] for the stainless steel tubular RHS and SHS X joint under axial compression. It was demonstrated that the design rules specified in CIDECT Design Guide No. 8 [4] for SCF of SHS and RHS tubular X joints overestimates the SCF.

2.5. SCFs at tubular K(N) joints

Fig. 16 shows a completely overlapped and a gapped tubular K(N) joint. These types of joints are common in offshore structures. Completely overlapped tubular joints are adopted to provide additional clearance where simple and partially overlapped joints are not desirable. In several places, it is not possible to brace a structural system with overlapped tubular joints throughout. In that case, gapped tubular joints are used to serve the purpose. However, overlapped tubular joints are found to have more strength than the gapped tubular joints.

Moe [53] studied stress distribution in overlapped K joint subjected to balanced axial loads. The maximum SCF was found to occur between crown and saddle of the lap brace,
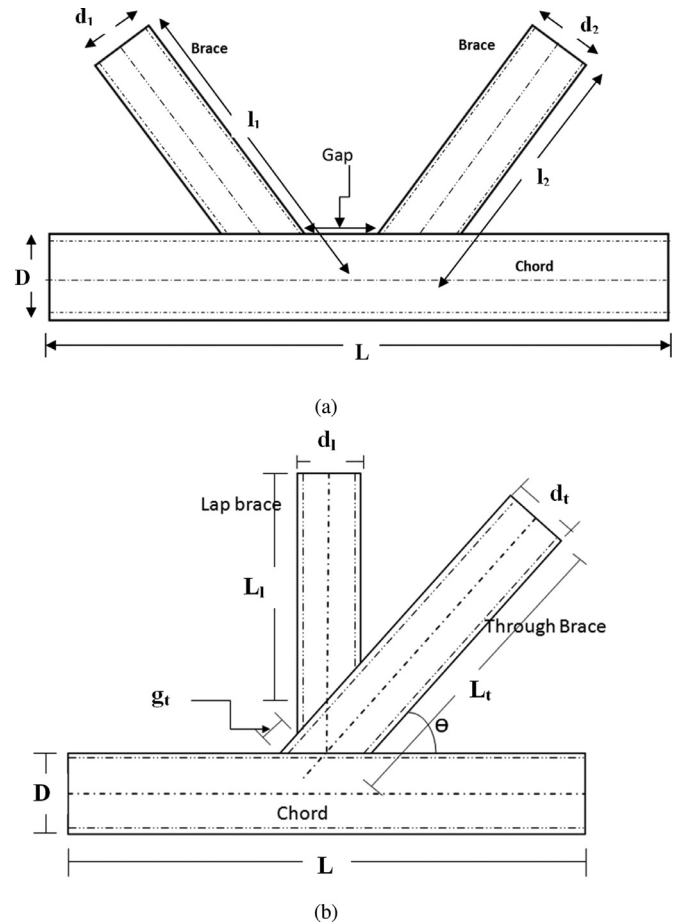
and crown heel and saddle of the through brace. A significant reduction in SCF was found when compared with the Kuang et al. [23] equations for gapped K joint. It was also mentioned that although SCF for overlapped K joint under balanced load case is smaller than the gapped K joint, it could be higher for the unbalanced load cases. Lalani and Forsyth [54] carried out experimental investigation on overlapped K(N) joint subjected to balanced load case. Using hot-spot stress approach, the maximum SCF was evaluated at the crown heel for the 45° diagonal brace and at crown position for brace perpendicular to the chord. It was found from their study that the maximum SCF need not necessarily occur at crown and saddle positions of the members.

Frater and Packer [55] tested two full scale warren trusses with welded gap K joint. They measured strain at three different connections with different weld sizes. The SCFs/SNCFs were calculated and were compare with the available parametric formulae. They concluded that the parametric formulae should consider the weld size as the experimental results were not consistent with the parametric equations. Wingerde et al. [56] carried out numerical study on K connections between SHS-SHS. They gave an overview of the finite element models and methods to determine SCFs and proposed a parametric equation based on large number of FE models between

geometric parameters and SCFs. This work contributed towards the general fatigue design guidelines for hollow structural sections.

Karamanos et al. [57] carried out finite element analysis of gapped K joints based on 20-node solid elements. SCFs were obtained at the joint intersection of the chord and the braces. The results covered various loading conditions such as in-plane bending, out-of-plane bending, balanced axial load and chord load. The hot-spot locations were identified and the carry over effects were studied in a rigorous manner. A set of design equations and graphs to estimate the SCFs of gapped tubular K joint were proposed in this work.

Gho et al. [58] tested a uni-planar completely overlapped K(N) joint to determine the hot-spot strains at the intersections for the verification of finite element model under lap brace axial loading. Experimental results showed that the maximum SCF occurs on the through brace saddle near the lap brace under axial loading. At the through brace saddle position, the strain concentration factor (SNCF) were found to be 2.84 and 2.77 from the experiment and FE analysis respectively. It was also concluded that completely overlapped tubular K joints cannot be considered as two separate Y joints. The existing parametric equations derived for T/Y joints overestimated the chord and through brace SCF by 13.7 and 8.66, respectively.

Shao [59] proposed a set of parametric equations to calculate SCFs in a gap tubular K joint under IPB load. The equations were derived from 1000 FE models after validating the model with the help of experimental results. The proposed equations were also validated with Morgan and Lee [33].

Gao et al. [60] proposed parametric equations to predict the SCF for the completely overlapped tubular K joints under in-plane bending. Numerical study based on thick shell elements and solid elements was performed. They tested a completely overlapped joint specimen for the verification of the finite element model. Linear method of extrapolation was adopted in both numerical and experimental study. This is because the strain distribution near the weld toe was found to be linear. A maximum of SNCF value of 1.73 was obtained at the crown heel of lap brace. There was an increase in SNCF from saddle to chord of members. An average difference of 10.7% was observed between the experimental SNCF values and SNCF obtained from the finite element analysis using 8 noded thick shell element. Based on the data of 5184 finite element models for completely overlapped joint, a parametric equation was proposed to determine the SCF at the crown toe and crown heel of through brace and lap brace.

Shao et al. [61] derived a set of parametric equations for the hot-spot stress distribution in a K joint under three basic loadings. It was concluded that based on these parametric equations, more accurate HSS prediction in tubular K joint subjected to any complex loading can be done using superposition principle.

Jiki [62] studied the stress concentrations in gapped tubular K joint using 20-noded isoparametric thin shell elements. It was proposed in this study that if the joint is gapped, then 50 mm should be the limit of spacing. This is because after 60 mm of spacing, alternating pattern of SCFs i.e., from positive to negative, were observed. It was found that the overlapped tubular K joints are stronger than the gapped tubular K joints.

Cao et al. [63] investigated the effect the welding residual stresses on the SCFs of K joints. Numerical simulation considering the thermo effect of welding process was carried out in ANSYS [64] employing the "element birth and death" technology. Stresses and temperature distributions were obtained while considering the changes in the material properties. Based on this model, the SCFs were calculated on two different models with and without welding residual stresses. By comparing the results from the two models, the difference in SCFs was found to be less than 10%. In addition, the effect of non-dimensional geometric parameters on the SCFs was also studied in detail.

Yang et al. [65] investigated the stress concentration in K(N) joints with negative large eccentricity under axial compressive loading. Finite element models were used to carry out parametric study after validating with 4 large scale test results. It was found that as the eccentricity decreases, the maximum SCF was found to shift from the saddle point to the crown point at the intersection of inclined brace and vertical brace.

2.6. SCFs at tubular KT and DKT joints

Tubular KT and DKT joints are frequently used in offshore structures. SCFs for these joints plays a crucial role in the evaluation of fatigue life of these structures. Ahmadi et al. [66] carried out the parametric study to predict the SCFs along the brace-to-chord intersection for the DKT joints under the balanced axial loads. The effect of non-dimensional parameters and brace to chord intersection on the distribution of SCFs. This was the first parametric equation proposed for DKT joints inspite of their frequent use in offshore structures. Ahmadi et al. [67,68], Ahmadi and Lotfollahi-Yaghin [69], Ahmadi and Zavvar [70], Ahmadi et al. [71,72] extensively studied the stress concentration phenomenon in internally ring-stiffened KT joints in offshore structures. Ahmadi et al. [67,68] carried out parametric study in internally stiffened KT joints subjected to balanced axial load, Ahmadi and Lotfollahi-Yaghin [69] for IPB, and Ahmadi and Zavvar [70] for OPB loading. Ahmadi et al. [71] derived probability density functions for the weld toe SCF in internally stiffened tubular KT joint subjected to axial loading. They demonstrated that the inverse Gaussian distribution is the most appropriate probability model for predicting the maximum value of SCFs in such joints.

2.7. SCFs at multi-planar tubular joints

Using finite element methods, Karamanos et al. [73] studied stress concentration in multi-planar tubular (CHS) XX joints (Fig. 2(b)) in steel structures under various loadings (including reference and carry-over loadings). The weld profile was modeled using 20 noded solid elements while the

brace and chord were modeled using 8 noded shell elements. The results were found to be in good agreement with the experimental results. It was concluded from their study that the saddle points and crown points are the most and least critical hot-spot locations, respectively.

Chiew et al. [74,75] tested a large-scale multi-planar XT joint and a large scale steel multi-planar tubular XX joint specimen with in-plane and out-of-plane braces subjected to a total of 12 different load cases. These load cases include the axial load and axial load combined with in-plane bending and out-of-plane bending. The experimental results were compared with the finite element simulations. Linear extrapolation was adopted to obtain the hot-spot strain. They identified the multi-planar effects when SCF results for multi-planar joints were compared with corresponding uni-planar joint. The authors characterized these effects as the multi-planar carry-over effect and multi-planar stiffness effect. Multi-planar carry-over effect was referred to as the load interference to the out-of-plane brace members from the loading on the in-plane brace members and vice versa. On the other hand, the total stiffness and load carrying capacity of the joints were found to be increased due to the presence of out-of-plane members. As a result, a decrease in stress concentration was observed for the loaded brace member and is referred as multi-planar stiffness effect. It was observed that the carry over effects are negligible under in-plane bending but dominant in case out-of-plane bending and to some extent, in axial loading. The multi-planar effects were found to be dependent on the load patterns and the relative geometrical location of the brace members.

Woghiren and Brennan [76] studied stress concentration in multi-planar rack-stiffened tubular KK/DK joints using finite element methods and proposed parametric equations. It was found that with the stiffness addition of rack plate, the SCF reduces significantly at the brace chord intersection but the new hot-spot locations were introduced.

Ahmadi et al. [77], Ahmadi and Lotfollahi-Yaghin [78], Ahmadi et al. [79,80] extensively studied the stress distribution near weld toe in multi-planar joints. Ahmadi et al. [77] derived parametric equations for SCF prediction of right angle two-planar DKT joint. The SCFs equations were given for outer (inclined) and central (vertical) braces of the DKT joint. Ahmadi and Lotfollahi-Yaghin [78] presented parametric equations to determine SCF on the chord-side saddle of central braces in three planar tubular KT joint. Ahmadi et al. [80] performed parametric stress analysis for 81 steel, two-planar, tubular DKT joints under two different axial loading conditions. The authors focused their study only on the central brace (because of relatively larger SCF) and studied the effect of various non-dimensional geometric parameters on the SCF values at the inner saddle, outer saddle and crown positions. After verifying the finite element analysis results with experimental data, a comprehensive database of SCF values were created based on finite element analysis. The developed SCF database covered three hot-spot locations (inner saddle, outer saddle, and crown) and two different axial load conditions. This database was then used to develop design
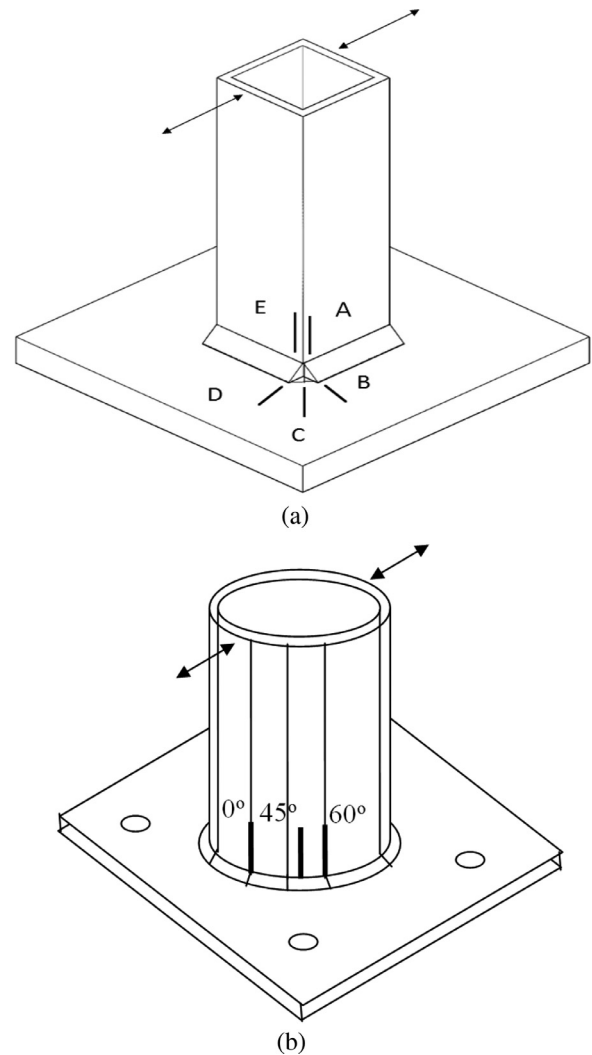

(a)

(b)

Fig. 17. Tubular to a Plate T joints: (a) Lines A–E where extrapolation for hot-spot stresses is recommended (Mashiri et al. [81]) and (b) Lines for hot-spot stress determination (Mashiri and Zhao [82]).

equations. From their study, a high difference was found to exist in the SCF values between SCF equation for equivalent uni-planer KT joints and multi-planar DKT joint. It was concluded that the equations for equivalent uni-planar KT joint would under-predict or over-predict the SCF for multi-planar DKT joint.

2.8. SCFs at tubular to a non-tubular section joints

Non-tubular joints such as flange joints (tubular to a flange joint) are widely used as continuity joints and for providing support in tubular joints in structures such as tubular trusses, communication towers, and road signal poles. Further, welded thin walled tubular to a plate T joint ($t < 4$ mm) made up of steel sections are used in various applications. Mashiri et al. [81] tested thin walled SHS to plate T joint under in-plane fatigue loading. They determined the SCFs along the lines A, B, C, D, E as shown in Fig. 17(a). The maximum SCFs were found to be 1.4–1.8 for line E. The ratio of the SCFs

determined using quadratic extrapolation to the SCFs using linear extrapolations at the hot-spot locations were found to be between 1.04 and 1.18. The authors concluded that the stress distribution at the hot-spot locations in the recommended region of extrapolation is non-linear.

Mashiri and Zhao [82] determined SCFs at different locations under in-plane bending for thin walled CHS to plate T joint along the weld toes on the tubular brace.The stress distribution around the weld toe shows that the highest SCF occurs at 0° line in the circular brace as shown Fig. 17(b). The magnitude of maximum SCFs in this investigation was found to be between 1 and 1.5 which was smaller than the maximum SCFs found in earlier studies of SHS to Plate T joint by Mashiri et al. [81].

Couchaux et al. [83] developed an analytical model based on elastic theory of thin plates and shells to determine the SCF at the toe of tube and flange weld in a tubular flange connection. This model was the extension of the work of Cao and Bell [84]. The work of Cao and Bell [84] did not account for the radial deformations and led to underestimation of SCF at the tube to flange connection. Couchaux et al. [83] considered the radial deformations. The numerical model was carried out in ANSYS [64]. Three-dimensional brick elements and contact elements were used for the analysis and the numerical results were compared with the experimental and analytical results. A quite good agreement was observed between numerical, analytical (Cao and Bell [84], Chabrolin and Ryan [85]) and the experimental results. It was concluded that the empirical formula developed by Chabrolin and Ryan [85] for the weld toe overestimates SCF for larger tube connections and underestimates for smaller tube connections.

Kršćanski and Turkalj [86] numerically investigated stress concentration in welded CHS-plate T joint. Finite element meshing was done as per the recommendations of Zhao and Packer [11]. Ten-node tetrahedral elements with modified formulations were used near the weld toe. The FE results were compared with the experimental results of Mashiri and Zhao [82] and found higher than the experimental values. However, the results were found to be consistent with different tube wall thickness and different loads.

3. Future research and challenges

From literature review, it may be observed that a significant progress has been made towards understanding the stress concentration in tubular joints. It is inferred from the literature that stress concentration is a complex problem in the context of hollow section tubular and non-tubular joints. This is because SCF depends on many factors, which are difficult to account accurately. Some of these are: (i) weld size effect, (ii) thickness of the brace and chord members, (iii) fixing the points of extrapolation, (iv) loading conditions in the brace and chord (v) type of material e.g., cold formed steel. Detailed studies are needed to evaluate SCF for different types of loading conditions in the brace and chord, and different combination of brace and chord sections. In case of non-tubular joints, research progress so far is minimal. Based

on this review, several issues that need immediate attention have been identified. These are listed as follows:

- One of the issue is the evaluation of stress concentration in the non-tubular joints, which are very common in the deck structure of template type fixed and floating type deep water (water depth >300 m) offshore platforms. As per the authors' knowledge, no design guidelines are available for the fatigue design of such non-tubular joints.

- The mesh insensitive structural stress method in evaluating SCF and fatigue life assessment is examined only for a few tubular joints. The structural stress method is needed to be validated for a wide range of tubular and non-tubular joint test data. Hence, parametric equation to evaluate SCF should be developed for various tubular and non-tubular joints, and different loading modes. It has been found that the new parametric equations derived using mesh insensitive structural stress approach are not conservative in relation with HSS *S-N* curves (Liu et al. [10]). Therefore, it is investigate the *S-N* curves corresponding to mesh insensitive structural stress.

- Another issue is the stress concentration in the welded thin walled tubular joints ($t < 4$ mm). Research done in this area indicates that wall thickness of tubular sections significantly affects the SCFs at the joint intersection, and thus, ignoring this effect will lead to overconservative design. The issues related to over-sized weld size effect and method of extrapolations for these joints are needed to be explored to develop proper design guidelines for fatigue design of welded thin walled tubular joints.

- The recommendations proposed so far, for overlapped tubular joints do not provide adequate idea about the fatigue design of these joints. In case of completely overlapped tubular joints, the angle of variation of lap brace with respect to the chord should be studied to determine the critical angle that causes the maximum SCFs at the joints. No information is available about the SCF of completely overlapped joints under out of plane bending and combined loading.

- The parametric equations and SCFs, which are currently used to determine the hot-spot stresses in tubular joints are mainly derived from the static load cases only. These equations do not differentiate between the dynamic (cyclic type or random) loading and static loading, which is very important (N' Diaye et al. [40]). Research is thus needed to study the influence of dynamic loading on the stress concentration factor of tubular and non-tubular joints. This will be highly useful for estimating fatigue life of these joints in offshore structure, where wave, ice and wind loads are very dominant.

- In case of square hollow section joints, the current fatigue design guidelines cover only the T/X, K(gap), K(overlap) joints. Thus, studies are required to be carried out for SHS joints, as they are more vulnerable to stress concentrations.

Many of the aforementioned issues can be studied through simulations. However, experiments must be conducted in

order to verify these findings, which may be a significant challenge. Ultimately the goal for the profession is to ensure a longer fatigue life for the tubular and the non-tubular joints employed in offshore and other structures. Hence, (i) development of simplified parametric equations to predict the SCF for tubular/non-tubular joints are required, which can be easily used by design engineers, and (ii) to reduce the stress concentration at the welded joints, some affordable and easily implementable techniques are needed to be developed. Undoubtedly, the availability of such equations and techniques will help in enhancing the fatigue performance of the tubular/non-tubular joints.

Acknowledgments

References

[1] A. Stacey, J. Sharp, in: Proceedings 8th International Conference on the behavior of Offshore Structures, 1994. Delft University of Technology, Delft, Netherlands
[2] E. Chang, W. Dover, Int. J. Fatigue 21 (4) (1999) 361–381.
[3] American Petroleum Institute (API), API RP 2A-WSD Recommended Practice for Planning, Designing and Constructing Fixed Offshore Platforms: Working Stress Design, American Petroleum Institute, Washington, D.C, 2005.
[4] X.L. Zhao, S. Herion, J.A. Packer, R. Puthli, G. Sedlacek, J. Wardenier, K. Weynand, A. van Wingerde, N. Yeomans, Design Guide for Circular and Rectangular Hollow Section Joints Under Fatigue Loading, Verlag TÜV Rheinland, Koln, Germany, 2000.
[5] D. Radaj, Design and Analysis of Fatigue-Resistant Welded Structures, Cambridge: Abington Publishers, 1990.
[6] A. Hobbacher, in: Recommendations for fatigue Design of Welded Joints and Components-International Institute of Welding, XIII-2151r4-07/XV-1254r4-07, IIW, Paris, 2008.
[7] A. Wingerde, J. Wardenier, J. Packer, J. Constr. Steel Res. 35 (1) (1995) 71–115.
[8] P. Dong, J. Offshore Mech. Arct. Eng. 127 (1) (2005) 68–74.
[9] P. Dong, J.K. Hong, J. Offshore Mech. Arct. Eng. 134 (3) (2012) 031602.
[10] G. Liu, X. Zhao, Y. Huang, Int. J. Fatigue 80 (2015) 216–230.
[11] X.L. Zhao, J.A. Packer, Fatigue Design Procedure for Welded Hollow Section Joints, International Institute of Welding documents XIII-1804-99 and IIW Document XV-1035-99, Abington Publishing, Cambridge, UK, 2000.
[12] D. Department of Energy, in: Background to New Fatigue Design Guidance for Steel Welded Joints in Offshore Structures, Report of the Department of Energy Notes Drafting Panel, Her Majesty's Stationery Office, 1984.
[13] American Welding Society (AWS), in: Structural Welding Code-steel, ANSI/AWS D1.1–2000, Miami, USA, 2000.
[14] American Petroleum Institute (API), API-PR2A Recommended Practice for Planning, Designing and Constructing Fixed Offshore Platforms, American Petroleum Institute, Dallas, USA, 1991.
[15] T. Gurney, Fatigue of Welded Structures, Cambridge University Press, Cambridge, UK, 1979.
[16] J. Wardenier, in: Hollow Section Joints, Delft University Press, Delft, The Netherlands, 1982.
[17] D. Radenkovic, in: Steel in Marine Structures, 1981, pp. 53–95. Paris, France
[18] Det Norske Veritas (DNV), in: Fatigue design of offshore steel structures, 2008 Recommended Practice DNV-RP-C203, Det Norske Veritas.

[19] W. Fricke, H. Petershagen, H. Paetzold, G. Lloyd, Fatigue Strength of Ship Structures. Part II: Examples, Germanischer Lloyd Aktiengesellschaft, 1998.
[20] W. Fricke, in: Proceedings of the 11th International Offshore and Polar Conference, 2001, pp. 40–47. Stavanger, Norway
[21] American Bureau of Shipping (ABS), in: Guide for Fatigue Strength Assessment of Tankers, Part 3 Steel Vessel Rules, American Bureau of Shipping, New York, 1992.
[22] A. Toprac, A. Beale, Weld. Res. Counc. 125 (1967) 1.
[23] J. Kuang, A. Potvin, J. Kahlich, Soc. Petrol. Eng. 1 (1) (1977) 287–299.
[24] A.C. Wordsworth, G.C. Smedley, in: European Offshore Steels Research Seminar, IX/P31, 1978, pp. 1–7.
[25] A.C. Wordsworth, in: Conf. on Fatigue In Offshore Structural Steel, I.C.E., London, 1981.
[26] Underwater Engineering Group, Design Guidance on Tubular Joints in Steel Offshore Structures, Report UR33, April, UK, 1985.
[27] M. Efthymiou, S. Durkin, in: Behavior of Offshore structures, Elsevier, Amsterdam, Netherlands, 1985.
[28] M. Efthymiou, in: Recent Development in Tubular Joints Technology, OTJ88, 1988. Surrey, UK
[29] A. Hellier, M. Connolly, W. Dover, Int. J. Fatigue 12 (1) (1990) 12–23.
[30] P. Smedley, P. Fisher, in: The First International Offshore and Polar Engineering Conference, (ISOPE), 1991, pp. 475–483. Edinburgh, UK
[31] M. Morgan, M. Lee, Int. J. Fatigue 19 (4) (1997) 309–317.
[32] M. Morgan, M. Lee, Int. J. Fatigue 20 (6) (1998) 449–461.
[33] M. Morgan, M. Lee, J. Struct. Eng., ASCE 124 (4) (1998) 382–390.
[34] UK Health and Safety Executive, in: Stress concentration factors for simple tubular joints- assessment of existing and development of new parametric formulae, OTH 354, Lloyd's Register of Shipping, London, UK, 1997.
[35] UK Health and Safety Executive, in: Stress concentration factors for tubular complex joints, OTH 91 353, Lloyd's Register of Shipping, UK, 1992.
[36] J. Buitrago, N. Zettlomoyer, J.L. Kohlich, in: Proceedings of the 16th Offshore Technology Conference, Paper No. 4775, 1984. Houston, Texas
[37] O. Dijkstra, R. Puthli, H. Snijder, J. Energy Resour. Technol., ASME 110 (1988) 246–254.
[38] R.d. borst, G.M.A. Kusters, P. Nauta, F.C.d. Witte, Finite Element Systems Handbook, Springer Verlag, Berlin, 1985. edition, Brebbia, C.A.,
[39] F. Mashiri, X. Zhao, P. Grundy, Int. J. Struct. Stab. Dyn. 4 (3) (2004) 403–422.
[40] A. N' Diaye, S. Hariri, G. Pluvinage, Z. Azari, Int. J. Fatigue 29 (8) (2007) 1554–1570.
[41] S. Yong-Bo, J. Constr. Steel Res. 63 (10) (2007) 1351–1360.
[42] J. Chen, J. Chen, W. Jin, J. Constr. Steel Res. 66 (12) (2010) 1510–1515.
[43] D.S. Ramachandra Murthy, A.G. Madhava Rao, P. Gandhi, P.K. Pant, J. Struct. Eng. 118 (11) (1992) 3016–3035.
[44] D.I. Nwosu, A.S.J. Swamidas, K. Munaswamy, J. Offshore Mech. Arct. Eng. 117 (2) (1995) 113–125.
[45] P.T. Myers, F.P. Brennan, W.D. Dover, Mar. Struct. 14 (4) (2001) 485–505.
[46] T. Fung, C. Soh, T. Chan, Erni, J. Struct. Eng., ASCE 128 (11) (2002) 1399–1412.
[47] A. Nazari, Z. Guan, W. Daniel, H. Gurgenci, Pract. Period. Struct. Des. Constr. 12 (1) (2007) 38–47.
[48] F. Mashiri, X. Zhao, P. Grundy, J. Struct. Eng., ASCE 128 (11) (2002) 1413–1422.
[49] L. Bian, J. Lim, J. Constr. Steel Res. 59 (5) (2003) 561–663.
[50] F. Mashiri, X. Zhao, P. Grundy, Eng. Struct. 26 (13) (2004) 1861–1875.
[51] L. Tong, H. Zheng, F. Mashiri, X. Zhao, J. Struct. Eng., ASCE 139 (11) (2013) 1866–1881.
[52] R. Feng, B. Young, J. Constr. Steel Res. 91 (0) (2013) 26–41.
[53] E. Moe, in: Steel in Marine Structures, 1987, pp. 395–404. Amsterdam, The Netherlands
[54] M. Lalani, P. Forsyth, in: Steel in Marine Structures, 1987, pp. 431–443. Amsterdam, The Netherlands
[55] G. Frater, J. Packer, J. Constr. Steel Res. 24 (2) (1993) 77–104.

[56] A. Wingerde, J. Packer, J. Wardenier, J. Constr. Steel Res. 43 (1û3) (1997) 87–118.

[57] S. Karamanos, A. Romeijn, J. Wardenier, Eng. Struct. 22 (1) (2000) 4–14.

[58] W. Gho, T. Fung, C. Soh, J. Struct. Eng., ASCE 129 (2003) 21–29.

[59] Y.B. Shao, Int. J. Space Struct. 19 (3) (2004) 137–147.

[60] F. Gao, Y. Shao, W. Gho, J. Constr. Steel Res. 63 (3) (2007) 305–316.

[61] Y.B. Shao, Z.F. Du, S.T. Lie, J. Constr. Steel Res. 65 (10) (2009) 2011–2026.

[62] P. Jiki, Modern Mech. Eng. 3 (2013) 50–54.

[63] Y. Cao, Z. Meng, S. Zhang, H. Tian, Appl. Ocean Res. 43 (2013) 195–205.

[64] ANSYS, V11.0 Documentation, ANSYS Inc, Canonsburg, PA,

[65] J. Yang, Y. Chen, K. Hu, Thin-Walled Struct. 96 (2015) 359–371.

[66] H. Ahmadi, M.A. Lotfollahi-Yaghin, M.H. Aminfar, J. Constr. Steel Res. 67 (8) (2011) 1282–1291.

[67] H. Ahmadi, M.A. Lotfollahi-Yaghin, S. Yong-Bo, M.H. Aminfar, Appl. Ocean Res. 38 (2012) 74–91.

[68] H. Ahmadi, M.A. Lotfollahi-Yaghin, S. Yong-Bo, Thin-Walled Struct. 70 (2013) 93–105.

[69] H. Ahmadi, M.A. Lotfollahi-Yaghin, Appl. Ocean Res. 51 (2015) 54–66.

[70] H. Ahmadi, E. Zavvar, Thin-Walled Struct. 91 (2015) 82–95.

[71] H. Ahmadi, A.H. Mohammadi, A. Yeganeh, Thin-Walled Struct. 94 (2015) 485–499.

[72] H. Ahmadi, A. Yeganeh, A.H. Mohammadi, E. Zavvar, Thin-Walled Struct. 99 (2016) 58–75.

[73] S.A. Karamanos, A. Romeijn, J. Wardenier, J. Constr. Steel Res. 50 (3) (1999) 259–282.

[74] S. Chiew, C. Soh, N. Wu, J. Struct. Eng., ASCE 125 (11) (1999) 1239–1248.

[75] S. Chiew, C. Soh, N. Wu, J. Struct. Eng., ASCE 126 (11) (2000) 1331–1338.

[76] C. Woghiren, F. Brennan, Int. J. Fatigue 31 (1) (2009) 164–172.

[77] H. Ahmadi, M.A. Lotfollahi-Yaghin, M.H. Aminfar, Thin-Walled Struct. 49 (10) (2011) 1225–1236.

[78] H. Ahmadi, M.A. Lotfollahi-Yaghin, J. Constr. Steel Res. 71 (2012) 149–161.

[79] H. Ahmadi, M.A. Lotfollahi-Yaghin, M.H. Aminfar, Thin-Walled Struct. 58 (2012a) 67–78.

[80] H. Ahmadi, M.A. Lotfollahi-Yaghin, M.H. Aminfar, J. Mar. Sci. Appl. 11 (1) (2012b) 83–97.

[81] F. Mashiri, X. Zhao, P. Grundy, L. Tong, Thin-Walled Struct. 40 (2) (2002) 125–151.

[82] F. Mashiri, X. Zhao, Thin Walled Struct. 44 (2) (2006) 159–169.

[83] M. Couchaux, I. Ryan, M. Hjiaj, in: Nordic Steel Construction Conference, 2009. Sweden

[84] J. Cao, A. Bell, Int. J.Press. Vess. Pip. 55 (3) (1993) 435–449.

[85] B. Chabrolin, I. Ryan, in: Tenue à la fatigue des pylônes de remontées mécanique, 1993. Rapport CTICM $N°$10 004–5

[86] S. Kršćanski, G. Turkalj, Eng. Rev. 32 (3) (2012) 147–155.